VIP Reaction Mechanisms

DOI: 10.1002/ange.201204833

Dihydrooxazine Oxides as Key Intermediates in Organocatalytic Michael Additions of Aldehydes to Nitroalkenes**

Gokarneswar Sahoo, Hasibur Rahaman, Ádám Madarász, Imre Pápai, Mikko Melarto, Arto Valkonen, and Petri M. Pihko**

The organocatalytic enantioselective Michael addition of aldehydes to nitroalkenes through enamine catalysis[1] has been studied intensively in recent years.[2] Pioneering mechanistic studies by Seebach and Hayashi and co-workers,[3] as well as by the Blackmond group,[4] on reactions catalyzed by diaryl prolinol ethers[5] have identified cyclobutane (CB) species **6a** (Scheme 1) as a key intermediate and the resting state of the amine catalyst. Although these studies clearly demonstrated that the rate-determining step in the catalytic cycle takes place after the formation of **6a**, and possibly involves the protonation of the iminium nitronate **5a**, the detailed mechanism of the rate-determining step was not addressed. More recently, the Blackmond group suggested a modified catalytic cycle where the cyclobutane species **6a** is first deprotonated to give the anion **10a**, followed by protonation to form the enamine **8a**.[4b]

Herein, we present a model derived from a combination of computational and experimental studies where the rate-determining step of the reaction involves protonation of the dihydrooxazine oxide (OO) species **11a** instead of the previously suggested species **5a**[3,4a] or **10a**.[4b] Furthermore, we demonstrate that the sluggish reaction rates observed in reactions with α-alkyl-substituted nitroalkenes (such as **4b)** are in fact due to slow protonation of the OO intermediate (e.g. **11b**; R = Me) and not a result of the intrinsically lower reactivities of the nitroalkenes. Finally, as a practical application of the insight obtained by these studies, we demonstrate that a simple *p*-nitrophenol co-catalyst remarkably accelerates reactions with α-alkyl nitroalkenes, to provide the products in synthetically useful yields and enantio- and diastereoselectivities.[6] The protonation of the dihydrooxazine oxide intermediate also explains the sense of diastereoselection of the protonation step.

At the outset, we decided to study the reaction with both α-unsubstituted and α-substituted nitroalkenes. Recently, Wennemers and Duschmalé[7] reported a tripeptide catalyst

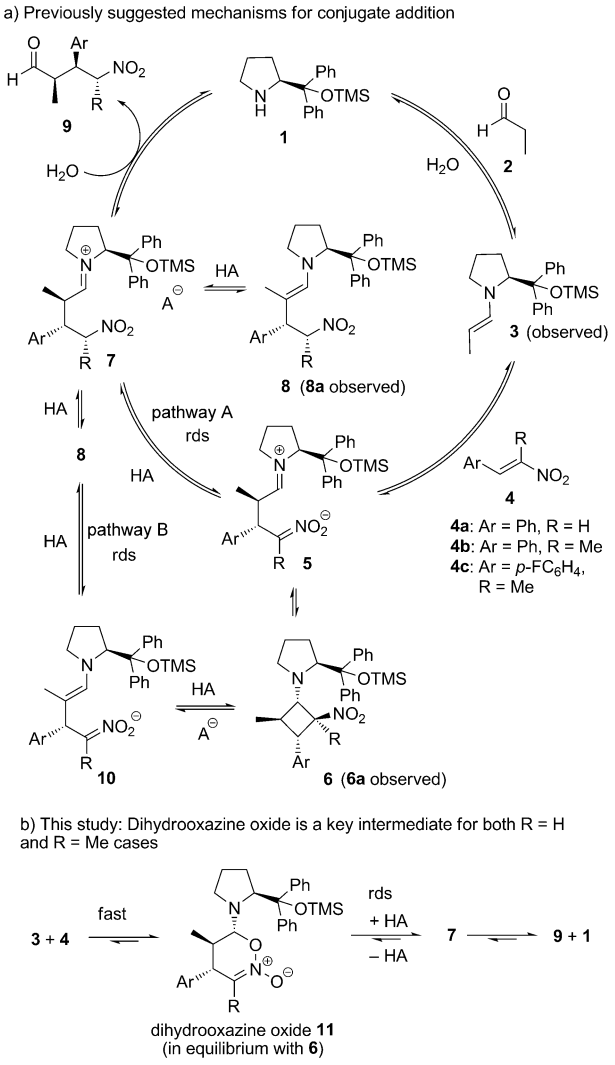

Scheme 1. Summary of the proposed mechanisms for the conjugate addition of aldehydes to nitroalkenes by enamine catalysis and the structure of the dihydrooxazine oxide species characterized in this study. Species labeled 'observed' have previously been identified and characterized by 1D and 2D NMR spectra and by HRMS.[3,4] rds = rate-determining step, TMS = trimethylsilyl.

[*] Dr. G. Sahoo, Dr. H. Rahaman, M. Melarto, Dr. A. Valkonen, Prof. Dr. P. M. Pihko
Department of Chemistry, Nanoscience Center
University of Jyväskylä, P. O. B. 35, FI-40014 JYU (Finland)
E-mail: Petri.Pihko@jyu.fi
Homepage: http://tinyurl.com/pihkogroup
Dr. Á. Madarász, Dr. I. Pápai
Institute of Organic Chemistry
Research Centre for Natural Sciences
Hungarian Academy of Sciences
P.O.B. 17, H-1525 Budapest (Hungary)
E-mail: papai@chemres.hu

[**] We thank Esa Haapaniemi and Mirja Lahtiperä for assistance with the NMR and HRMS measurements, respectively. This work was supported by the Academy of Finland (project Nos. 123813 and 138854 to P.M.P.), the Hungarian Research Foundation (OTKA, Grant NN-82955), and COST CM0905. A.V. thanks Academy Prof. Kari Rissanen for funding through the Academy of Finland (KR project Nos. 130629, 122350, and 140718).

Supporting information for this article is available on the WWW under http://dx.doi.org/10.1002/anie.201204833.

that provides acceptable reaction rates and excellent enantioselectivities for reactions with α-alkyl nitroalkenes, such as **4b**. They suggested that the lower reactivity of **4b** is a result of suboptimal conjugation of the phenyl ring with the nitroalkene. If, however, the turnover-limiting step occurs later in the catalytic cycle, as suggested by the groups of Seebach, Hayashi, and Blackmond for **4a**,[3,4] the lower reactivity of α-alkyl nitroalkenes might not be related to the reactivity of the starting nitroalkene at all. Instead, we should consider the reactivity of the intermediates. To resolve this issue, we decided to investigate the reactions with both **4a** and **4b** by a combination of computational and experimental studies.

Our initial computational analysis[8] focused on the identification of the reaction intermediate formed upon the C–C bond formation process between enamine **3** and nitroolefin **4a**.[9] We found that the conjugate addition leads to spontaneous ring closure between the oxygen atom of the nitro group and the iminium carbon atom resulting in an OO species (**11a**). The zwitterionic iminium nitronate **5a** could not be located as a low-lying energy minimum on the potential energy surface even with the inclusion of solvent effects. The computations also showed that **11a** can easily transform into CB **6a** in a single step. Similar results were obtained for the addition of enamine **3** to α-substituted nitroolefin **4b**. The energetics of these transformations are illustrated in Figure 1.

Based on these results, it is very unlikely that the zwitterion **5** is involved in the catalytic cycle, but instead, the OO species **11** may play a key role, presumably in the protonation step. **11** is predicted to be in a rapid equilibrium with CB **6** for both reactions, but notable differences are seen in their relative stabilities for the R = H and R = Me cases. In the reaction with **4a** (R = H), the cyclobutane **6a** is favored thermodynamically, whereas the stability order is reversed for **6b**/**11b** (R = Me), as the OO species **11b** is favored.[10]

Guided by these computational findings, we embarked on the experimental study of the reaction progress, with the hope of identifying the OO species **11a** and/or **11b**.[11] Figure 2 shows the conversion versus time profile for the reaction between **2** and **4a** with an excess of catalyst **1**. The initial spike of the CB formation (**6a**; blue curve) and the conversion into

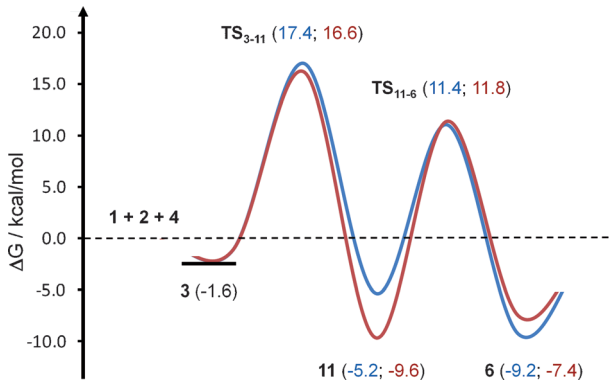

Figure 1. Free-energy diagram computed for the reactions of enamine **3** with nitroalkanes **4a** (R = H; blue) and **4b** (R = Me; red). Relative solution-phase Gibbs free energies (in kcal mol^{-1}; with respect to reactants **1** + **2** + **4**) are given in parentheses.[8]

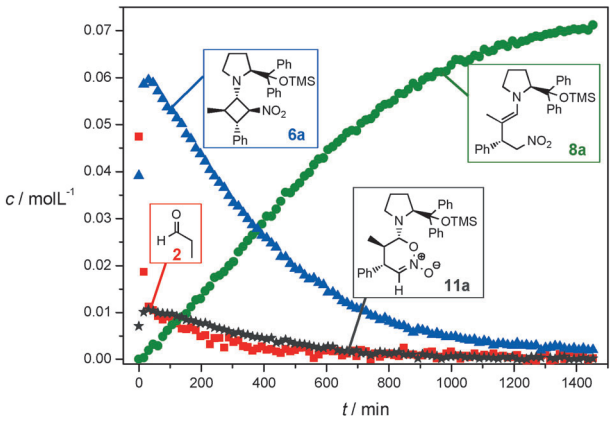

Figure 2. A plot of concentration versus time for different species in the reaction between **2** and **4a** in [D_8]toluene with an excess of **1**. Reaction conditions: $[\mathbf{2}]_0$ and $[\mathbf{4a}]_0 = 0.086$ M, $[\mathbf{1}]_0 = 0.172$ M (see the Supporting Information for more details).

the product enamine **8a** (green curve) are both in line with previous studies.[3,4] Importantly, however, we also observed a second minor intermediate (dark grey curve) that appears to form and decay contemporaneously with the cyclobutane **6a**, thus indicating that these species are linked together and likely involved in a rapid equilibrium. This new species was confirmed to be the dihydrooxazine oxide **11a** by 2D NMR experiments (COSY, HMQC; see the Supporting Information).[12]

When the corresponding reaction with **4b** was monitored, the analogous OO species **11b** was observed by NMR spectroscopy, but the cyclobutane **6b** was not detected. This result confirmed the computationally predicted stability order between **11b** and **6b**. In the absence of added acid, **11b** was stable for hours (see Figure 3), and its identity could be established by an array of NMR experiments (COSY, NOESY, HMQC, HMBC) as well as by HRMS (see the Supporting Information). The similarity between the ^{1}H NMR spectra of **11a** and **11b** provides further evidence for their identity (see the Supporting Information).

When the reaction between **2** and **4b** was carried out with 40 mol% of **1**, addition of acid *p*-nitrophenol (**12**) caused the linear decay of aldehyde **2** and concomitant linear increase in the concentration of the product aldehyde **9b** (Figure 3). The concentration of the OO species **11b** remained constant during this time, suggesting that it is a steady-state intermediate. Similar observations were made when the reaction was carried out in $CDCl_3$, and in experiments with nitroalkene **4c** (Ar = *p*-FC_6H_4). From **4c**, we obtained a third OO species **11c**, which was also fully characterized by 2D NMR spectroscopy and HRMS (see the Supporting Information).

A set of control experiments were conducted to probe the reversibility of the formation of **11**. First, experiments starting from aldehyde **9c** and catalyst **1** in the presence or absence of *p*-nitrophenol led to the formation of **11c** and the product enamine **8c**, thus confirming that **11c** is a thermodynamically stable species that can also be generated from the product (Figure 4a).

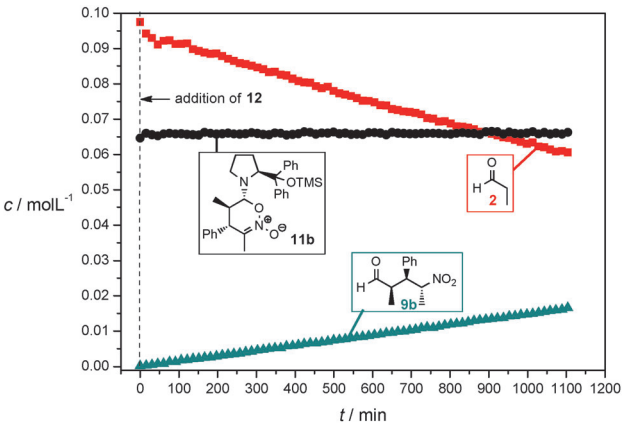

Figure 3. A plot of concentration versus time for different species in the reaction between **2** and **4b** in [D_8]toluene. Reaction conditions: $[\mathbf{2}]_0$ and $[\mathbf{4b}]_0 = 0.172$ M, $[\mathbf{1}]_0$ and $[\mathbf{12}]_0 = 0.068$ M (see the Supporting Information for more details).

The dynamic exchange between the CB species **6a** and the OO species **11** was established by crossover experiments where either nitroalkene **4b** or **4c** was added to a reaction mixture containing a maximum concentration of **6a**/**11a** (Figure 4b and c). These experiments revealed that the decay

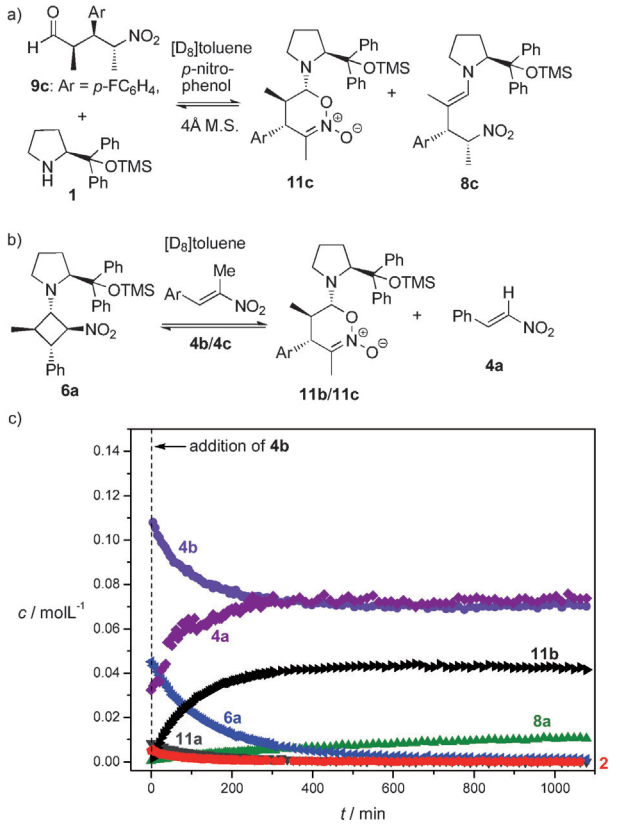

Figure 4. a) Reversibility experiments. b) Crossover experiments. c) A plot of concentration versus time for the crossover experiment starting from cyclobutane **6a** and α-alkylnitroalkene **4b**, showing the dominance of the dihydrooxazine oxide species **11b**. For reaction conditions, see the Supporting Information. M.S. = molecular sieves.

of the CB species **6a** and the decay of **11a** are accompanied by a steady increase in the concentration of either **11b** (see Figure 4c) or **11c**, but the product enamine (**8a**) was generated only slowly. A complementary crossover experiment starting from **11b** and **4a** led to a very slow but steady formation of product enamine **8a** and a slow decay of **11b** (see the Supporting Information). The crossover experiments demonstrate that the CB and OO species are involved in a dynamic equilibrium and they can revert into the reactants, albeit at a slow rate. The presence of the methyl group α to the nitro group (as in **11b** and **11c**) renders the OO species more stable relative to CB and no CB species corresponding to **11b** or **11c** could be detected. The OO species **11b** and **11c** are so stable that they convert into products only upon the addition of *p*-nitrophenol or upon the addition of nitrostyrene (**4a**), which traps the enamine **3** that is slowly released in a reversible reaction from **11b**, thus providing an exit via the formation of product enamine **8a.**

To gain further mechanistic insight into the protonation step of the catalytic cycle, reaction pathways corresponding to the protonation of **6a**/**6b** and **11a**/**11b** with *p*-nitrophenol (**12**) were explored computationally and other alternative pathways were considered as well (see the Supporting Information). Our results indicate that the protonation takes place preferentially on the C3 carbon of the OO species, and the attack on the *Si* face of the six-membered ring was found to be clearly favored kinetically (see Figure 5). The computations

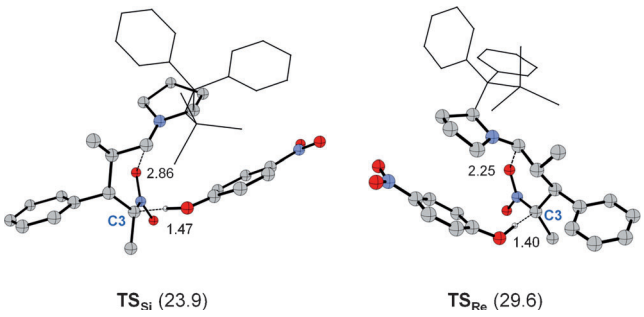

Figure 5. Diastereoselective protonation of intermediate **11b**. Protonation barriers (in kcal mol^{-1}, with respect to the **11b**···**12** adduct) are given in parenthesis. Bond distances indicated by dashed lines are given in Å. For clarity, all hydrogen atoms (except those involved in the proton transfer) are omitted, and the bulky CPh_2OTMS group of the catalyst is represented by simple lines. Blue N, red O.

thus predict diastereoselective protonation for reactions with α-substituted nitroalkanes. The diastereoselectivity appears to be governed by differential stabilizing electrostatic interactions in the iminium–phenolate ion-pair intermediate (see the Supporting Information). The free-energy barriers of protonation for the reactions with **4a** and **4b**, are calculated to be 20.6 and 23.9 kcal mol^{-1}, respectively; these values are consistent with the observed reaction rates. The nature of the protonation transition states indicates that the barriers arise predominantly from the ring opening of the OO species.[13] As a result of the enhanced stability of **11b** relative to **11a**, the ring opening is less favored for **11b**, thus resulting in a larger kinetic barrier for the protonation process. The iminium

intermediate **7a** or **7b** is deprotonated by the conjugate base of **12** to form enamine **8a** or **8b** (see the Supporting Information for computational details of this process).

α-Alkyl nitrostyrenes such as **4b**, and α-alkyl nitroalkenes in general, have been perceived as a challenging substrate class for enamine-catalyzed conjugate additions.[7,14] We now offer an explanation why this is the case: the resulting OO intermediates (e.g. **11b**) are very stable and convert into products only with the addition of acid, such as **12**.

The fact that **12** restores catalytic activity is synthetically useful, and we also explored briefly the preparative value of this simple protocol using 10 mol% of catalyst **1** and 40 mol% of **12**. Further solvent and additive screens indicated that **12** is indeed an optimal co-catalyst, and somewhat faster rates are obtained for reactions in $CHCl_3$ rather than those in toluene. Under these reaction conditions, a variety of aldehydes **2** and α-alkyl nitroalkenes **4** were screened (Table 1).

Table 1: Enantio- and diastereoselective Michael addition of aldehydes to α-alkyl nitro alkenes.[a]

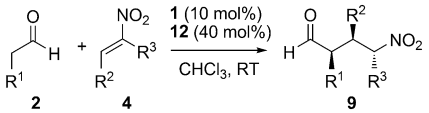

2 **4** **9**

Entry	R^1	R^2	R^3	*t* [h]	Yield [%][b]	d.r.[c]	e.r.[d]
1	Me	Ph	Me	30	68[f]	92:7:1:<1	>99.5:<0.5
2	*n*Bu	Ph	Me	25	94	90:6:4:<1	>99.5:<0.5
3	nC_8H_{19}	Ph	Me	24	94	89:7:4:<1	>99.5:<0.5
4	Me	*p*-FC_6H_4	Me	23	70[f]	92:8:<1:<1	>99.5:<0.5
5	*n*Bu	*p*-FC_6H_4	Me	21	93	92:6:2:<1	>99.5:<0.5
6	nC_8H_{19}	*p*-FC_6H_4	Me	18	85	89:10:1:<1	>99.5:<0.5
7	Me	*p*-ClC_6H_4	Me	21	71[f]	84:1:15:<1	>99.5:<0.5
8	*n*Bu	*p*-ClC_6H_4	Me	17	94	91:6:3:<1	>99.5:<0.5
9	*n*Hex	*p*-ClC_6H_4	Me	18	93	91:6:3:<1	>99.5:<0.5
10	Me	*p*-tolyl	Me	24	63[f]	91:1:8:<1	>99.5:<0.5
11	*n*Bu	*p*-tolyl	Me	27	84	90:6:4:<1	>99.5:<0.5
12	nC_8H_{19}	*p*-tolyl	Me	25	87	90:6:4:<1	>99.5:<0.5
13	*n*Bu	Ph[e]	Et	61	92	85:15:<1:<1	>99.5:<0.5
14	nC_8H_{19}	Ph[e]	Et	65	89	83:17:<1:<1	>99.5:<0.5

[a] Reaction conditions: **2** (200 mol%), **4** (100 mol%), **1** (10 mol%), **12** (40 mol%). [b] Yields are of the isolated aldehyde. [c] Determined by ^{1}H NMR spectroscopy. [d] e.r. was determined by HPLC analysis of the corresponding enoate or the derived alcohol (see the Supporting Information for details). [e] With 300 mol% of **2** and 80 mol% of **12**. [f] The product aldehyde is volatile.

The products were isolated in good to excellent yields, and in all cases the isolated products displayed excellent enantioselectivities (>99.5:<0.5 e.r. in all tested cases) and typically good diastereoselectivities for the *syn*, *anti* product **9**.[15] The experimental diastereoselectivity of the protonation step matches that predicted by the computational studies, thus providing another cross-check for the protonation mechanism emerging from the computations.

In conclusion, we present here spectroscopic and computational evidence that dihydrooxazine oxides (OO) are key on-cycle intermediates in the Michael additions of aldehydes to nitroalkenes catalyzed by diaryl prolinol ethers. The previously identified cyclobutanes and the OO species can rapidly interconvert, but the computations indicate that only the OO species are on the catalytic cycle and become protonated in the rate-determining step. The experimentally observed stability of the OO species explains the sluggish reaction rates observed with α-alkyl nitroalkenes, and this obstacle can be overcome with a suitable choice of an acid co-catalyst, to afford the products with high enantio- and diastereoselectivities. The observed stereoselectivity of the protonation step is consistent with the computational model. A revised catalytic cycle is presented in Scheme 2.

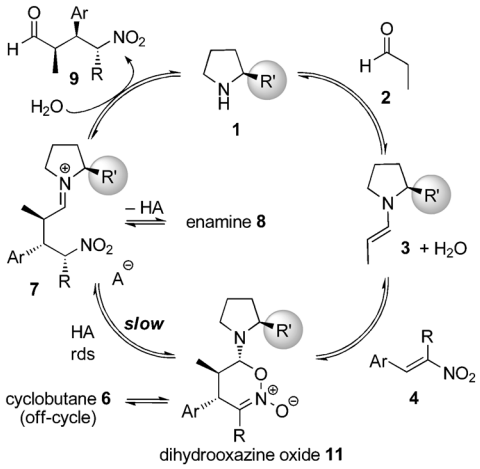

Scheme 2. Revised mechanism for the Michael addition of aldehydes to nitroalkenes catalyzed by **1**.

An important lesson of this study is that significant differences in reaction rates with different substrates can also result from differential stability of the intermediates, and different intermediates may dominate even in seemingly similar reactions. Fortunately, the experimental and especially the computational tools to characterize the intermediates have now advanced to a level where their combined use can provide a very detailed picture of the catalytic reactions, and offer synthetically relevant insights.

Received: June 20, 2012
Revised: October 10, 2012
Published online: November 13, 2012

Keywords: aminocatalysis · computational chemistry · heterocycles · intermediate characterization · NMR spectroscopy

[1] For reviews of enamine catalysis, including a discussion of different activation modes, see: a) A. Erkkilä, I. Majander, P. M. Pihko, *Chem. Rev.* **2007**, *107*, 5416; b) S. Mukherjee, J. W. Yang, S. Hoffmann, B. List, *Chem. Rev.* **2007**, *107*, 5471; for a detailed NMR study of enamine intermediates derived from **1**, see: c) M. B. Schmid, K. Zeitler, R. M. Gschwind, *Chem. Sci.* **2011**, *2*, 1793.

[2] For recent reviews, see: a) P. Melchiorre, M. Marigo, A. Carlone, G. Bartoli, *Angew. Chem.* **2008**, *120*, 6232; *Angew. Chem. Int. Ed.*

2008, *47*, 6138; b) S. Bertelsen, K. A. Jørgensen, *Chem. Soc. Rev.* **2009**, *38*, 2178; c) C. Palomo, A. Mielgo, *Angew. Chem.* **2006**, *118*, 8042; *Angew. Chem. Int. Ed.* **2006**, *45*, 7876; d) S. Sulzer-Mossé, A. Alexakis, *Chem. Commun.* **2007**, 3123.

[3] K. Patora-Komisarska, M. Benohoud, H. Ishikawa, D. Seebach, Y. Hayashi, *Helv. Chim. Acta* **2011**, *94*, 719, and references therein.

[4] a) J. Burés, A. Armstrong, D. G. Blackmond, *J. Am. Chem. Soc.* **2011**, *133*, 8822; b) J. Burés, A. Armstrong, D. G. Blackmond, *J. Am. Chem. Soc.* **2012**, *134*, 6741; corrigendum (for the assignment of **10a**): J. Burés, A. Armstrong, D. G. Blackmond, *J. Am. Chem. Soc.* **2012**, *134*, 14264.

[5] a) Y. Hayashi, H. Gotoh, T. Hayashi, M. Shoji, *Angew. Chem.* **2005**, *117*, 4284; *Angew. Chem. Int. Ed.* **2005**, *44*, 4212; b) J. Franzén, M. Marigo, D. Fielenbach, T. C. Wabnitz, A. Kjaersgaard, K. A. Jørgensen, *J. Am. Chem. Soc.* **2005**, *127*, 18296.

[6] For a previous study on the effect of H-bond co-catalysts in these reactions, see: H. Rahaman, Á. Madarász, I. Pápai, P. M. Pihko, *Angew. Chem.* **2011**, *123*, 6247; *Angew. Chem. Int. Ed.* **2011**, *50*, 6123.

[7] J. Duschmalé, H. Wennemers, *Chem. Eur. J.* **2012**, *18*, 1111.

[8] DFT calculations were carried out using the dispersion-corrected range-separated hybrid ωB97X-D functional. The 6–311G(d,p) basis set was used for geometry optimizations, vibrational analysis, and the estimation of solvent effects, whereas the electronic energies were obtained in single-point energy calculations using the large 6-311++G(3df,3pd) basis set. The solvation free energies (in chloroform) were computed by using the SMD continuum model. The reported energies refer to solvent-phase Gibbs free energies. For further details, see the Supporting Information.

[9] The C–C bond formation step between **3** and **4a** was investigated in previous computational studies, however, intermediates related to the identified transition states were not discussed, see: a) C. B. Shinisha, R. B. Sunoj, *Org. Biomol. Chem.* **2008**, *6*, 3921; b) J.-Q. Zhao, L.-H. Gan, *Eur. J. Org. Chem.* **2009**, 2661.

[10] The enhanced stability of **11b** relative to **11a** arises from the electron-donating properties of the α-methyl substituent; in contrast this group destabilizes the four-membered ring structure in **6b**. For a detailed analysis, see the Supporting Information.

[11] For previous studies on dihydrooxazine oxides, see: a) F. Felluga, P. Nitti, G. Pitacco, E. Valentin, *Tetrahedron* **1989**, *45*, 2099; b) F. Felluga, P. Nitti, G. Pitacco, E. Valentin, *J. Chem. Soc. Perkin Trans. 1* **1992**, 2331; for a suggestion of the OO species as a reversible catalyst sink, see: c) M. P. Lalonde, Y. Chen, E. N. Jacobsen, *Angew. Chem.* **2006**, *118*, 6514; *Angew. Chem. Int. Ed.* **2006**, *45*, 6366.

[12] During the reviewing of this manuscript, **11a** and other 1,2-oxazine N-oxides were independently identified by Seebach et al.: D. Seebach, X. Sun, C. Sparr, M.-O. Ebert, W. B. Schweizer, A. K. Beck, *Helv. Chim. Acta* **2012**, *95*, 1064.

[13] The protonation of the OO species **11a** and **11b** takes place in concert with ring opening, but the two events are asynchronous. The protonation process begins with the ring opening, which renders the C3 carbon more basic and facilitates the proton transfer from the phenolic OH. For further details, see the Supporting Information.

[14] For previous examples with cyclic nitroalkenes, see: a) L. Guo, Y. Chi, A. M. Almeida, I. A. Guzei, B. K. Parker, S. H. Gellman, *J. Am. Chem. Soc.* **2009**, *131*, 16018; b) B. Stevenson, W. Lewis, J. Dowden, *Synlett* **2010**, 672; with nitroalkenes bearing additional hydrogen-bond-donor groups: c) Y. Wang, S. Zhu, D. Ma, *Org. Lett.* **2011**, *13*, 1602; for a very recent example with acyclic α-alkylnitroalkenes with a benzoic acid co-catalyst, see: d) L. Wang, X. Zhang, D. Ma, *Tetrahedron* **2012**, *68*, 7675.

[15] The stereochemistry of **9b** was confirmed by X-ray analysis. CCDC 884143 contains the supplementary crystallographic data for this paper. These data can be obtained free of charge from The Cambridge Crystallographic Data Centre via www.ccdc.cam.ac.uk/data_request/cif.

